Scanning Electron Microscopy

Volume 1985 | Number 3 Article 8

7-21-1985

Scanning Acoustic Microscopy in Materials Characterization

H. R. Vetters
Stiftung Institut fuer Haerterei-Technik

P. Mayr
Stiftung Institut fuer Haerterei-Technik

S. Boseck
Stiftung Institut fuer Haerterei-Technik

Th. Luebben
Stiftung Institut fuer Haerterei-Technik

R. Matthaei
Stiftung Institut fuer Haerterei-Technik

See next page for additional authors

Scanning Acoustic Microscopy in Materials Characterization

Authors

H. R. Vetters, P. Mayr, S. Boseck, Th. Luebben, R. Matthaei, and A. Schulz

SCANNING ELECTRON MICROSCOPY/1985/III (Pages 981-989)
SEM Inc., AMF O'Hare (Chicago), IL 60666-0507 USA

0586-5581/85$1.00+.05

SCANNING ACOUSTIC MICROSCOPY IN MATERIALS CHARACTERIZATION

H.R. Vetters, P. Mayr*, S. Boseck, Th. Luebben, R. Matthaei, A. Schulz+

Stiftung Institut fuer Haerterei-Technik,
Bremen Lesumer Heerstr. 32, D-2820 Bremen 77, FRG

+Universitaet Bremen, Fachbereich Physik
D-2800 Bremen, FRG

(Paper received February 27, 1985: manuscript received July 21, 1985)

Abstract

The scanning acoustic microscopy is a powerful tool for subsurface imaging and therefore fault detection in coated parts. In this paper several methods are established to reveal the imaging of hidden structures. First efforts were made to find out the information depth due to the various distances between lens and surface of the object. By means of a specially developed test specimen it was possible to estimate the penetration depth for monitoring structural details. The indepth analysis of layered composites is considered by the determination of the V(z)-characteristics. Furthermore the gain of image processing by means of Fourier transformed patterns and simultaneous filtering is shown by a typical example.

KEY WORDS: Scanning acoustic microscopy, Indepth analysis, Analysis of hidden structures, Non-destructive microbeam analysis, Acoustic wave monitoring

*Address for correspondence:
Stiftung Institut fuer Haerterei-Technik
Lesumer Heerstr. 32, P.O.B. 77 02 07
D-2820 B r e m e n 77, F.R.G.
Phone No.(0421) 630007

Introduction

Scanning acoustic microscopy (SAM) is gaining importance as new analytical tool for non-destructive materials testing. One of the most significant benefits of SAM is providing indepth examination due to the sound-transparency of solid material [1,7] forming simultaneously ultrasonic images. The present contribution deals with the study of the indepth analysis and the level of information provided by acoustic micrographs obtained by SAM. The method developed by Lemons and Quate [5] routines as follows. A radio frequency oscillation - - formed to a pulse of defined width - is passed through a piezoelectric transducer which generates ultrasonic waves of the same frequency. These acoustic waves pass a sapphire lens and are transformed into spherical acoustic waves. This is realized by means of a small concave surface at the tip of the lens (Fig. 1)

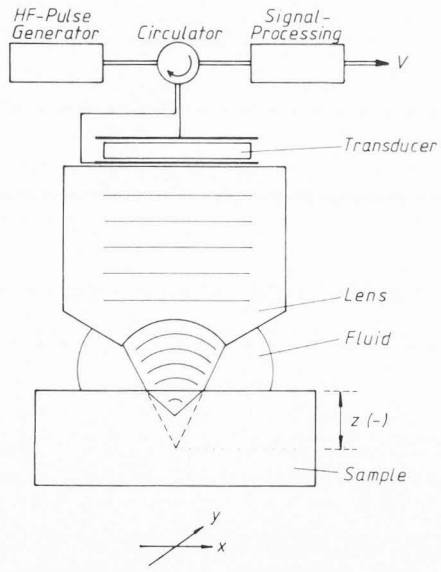

Fig. 1 SAM-reflective mode system

An immersion medium, for example water, fills the gap between the lens and the object in order to provide a path for ultrasound propagation. The acoustic sapphire lens has few spherical aberrations due to the magnitude ratio of the ultrasound velocities of the sapphire and water. This facilitates the good convergence of the sound waves on the specimen. The lateral resolution on the surface is limited by diffractive properties. The acoustic waves reflected by the specimen are collected by the same acoustic lens and converted into an electric signal by the piezoelectric transducer. Suitable electronic circuits are used to separate the reflected pulse from the incident pulse and noise, and the intensity of a pixel on the monitor (CRT) is obtained. A full image can be received by scanning the specimen with the mechanically oscillating acoustic lens and by simultaneous perpendicular movement of the motor driven specimen support mounted below the lens. The investigations described are carried out with an ultrasound frequency of 200 MHz. The immersion medium is distilled water. The commercially available instrument operates for reflective optical and scanning acoustic microscopy [9] .

A characteristic parameter of SAM is the output voltage V(z) as a function of the displacement (z). This value is used to describe the acoustic material properties [1,5,7]. Focusing on the surface is defined as z=0 where the maximal value of V(z) is obtained. A reduction of the gap between lens and specimen surface is indicated by negative z-values. It should be mentioned that the z-index values do not refer directly to the positions of the reflection plane below the surface. The different intensities recorded on the CRT are due to the V(z)-characteristics which depend on elastic properties of the material [1,5,7]. In crystalline solids the V(z)-graphs are also influenced by the crystallographic orientation [8] as well as by residual stresses.

Characterization of the Microstructure

Acoustic imaging may be useful to develop the microstructure of unetched metallic objects. For example the heat influenced zone of a resistance spotwelded junction shows a typical structure revealed by means of SAM. The acoustomicrograph (Fig.2) of the polished but unetched cross section of the welding spot indicates the various crystal domains in the heat affected area. It is demonstrated that the main problem-to separate the fine grained regions at the seam of the melting zone and the dendritic structure in the center-can be solved easily. The benefit of non-etching and the detection of different elastic material parameters provide more detailed information than those which can be obtained by means of optical microscopes.

Indepth Analysis of Layered Composites

The transparency of most materials to sound permits an indepth examination of samples. By showing hidden defects, flaws or subsurface cracks the SAM proves to be used for subsurface analysis

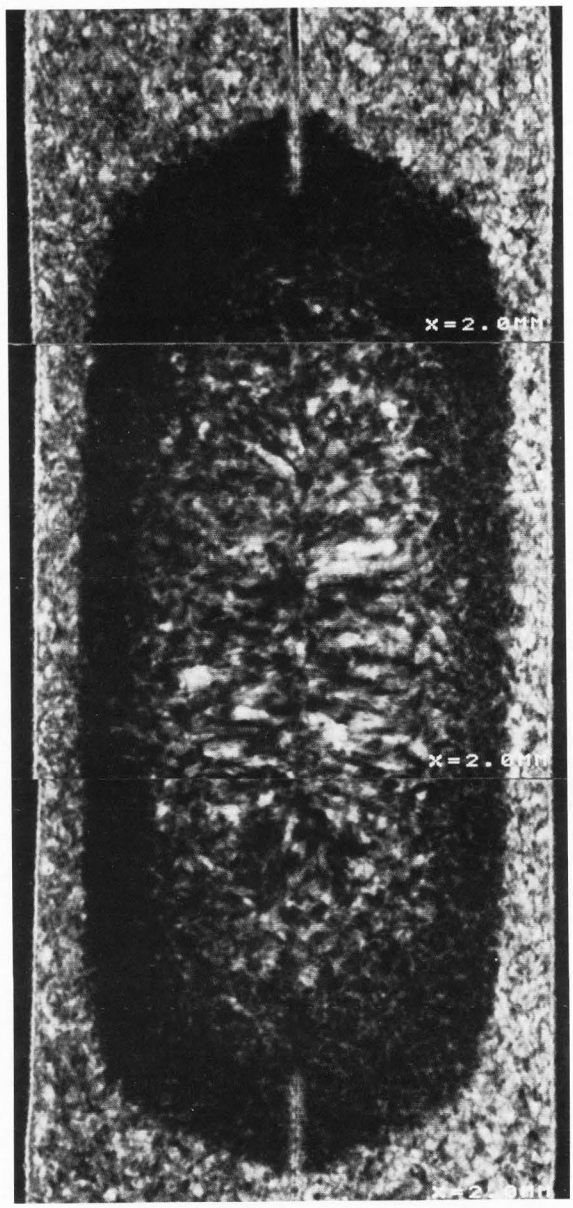

Fig. 2 Cross section of a spot welded junction. The slits mark the interface of the two welded sheets. Acoustomicrograph of the unetched polished surface.

⟼ = 100 µm

in coated parts [2,4] or in diffusion-bondings. To verify information about the subsurface detection it is necessary to determine the penetration depth of acoustic wave monitoring. The analysis of a well defined hidden structure seems to be a helpful approach to estimate the parameters mentioned above.To demonstrate the feasibility of this a mesh grid (nickel) was fixed below an aluminium foil by a cover of epoxy resin [6] as shown in Fig. 3.

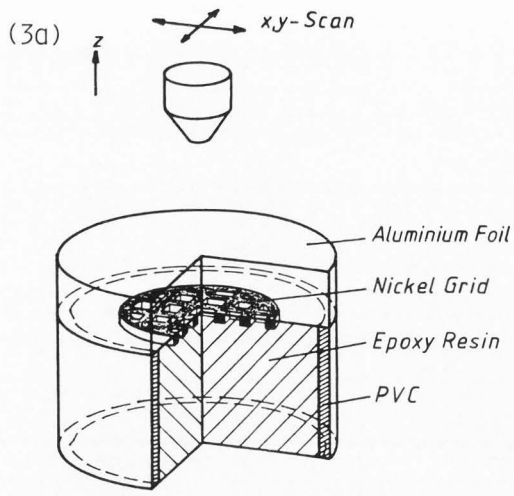

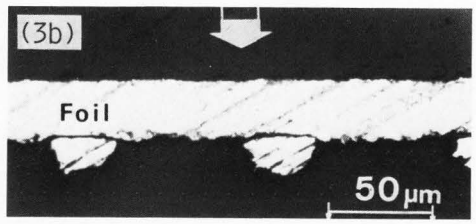

Fig. 3 Test specimen for subsurface imaging

The foil-thickness is 30 µm, the grid has 78.74 mesh per cm and one gridline is 42 µm wide with a thickness of about 25 µm. Fig. 4 shows a series of acousto-micrographs at various displacement steps.

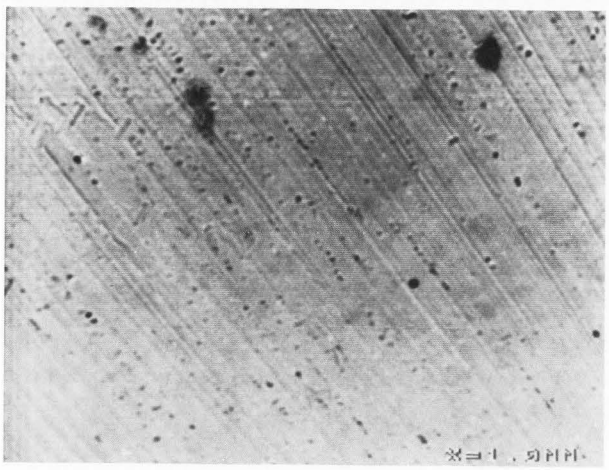

Fig. 4a SAM micrograph of the test specimen, z = 0, aluminium layer on the top. ⟵⟶ = 100 µm

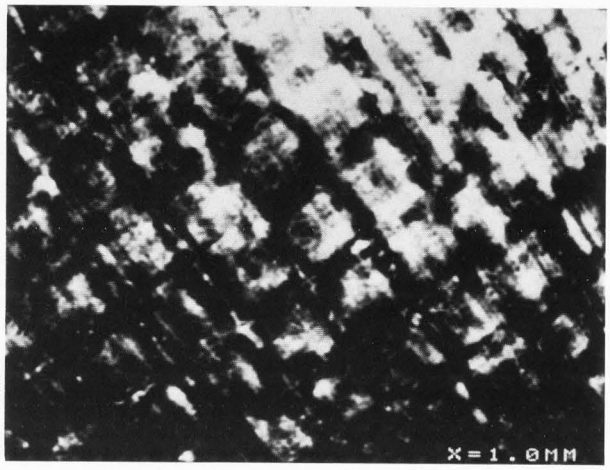

Fig. 4b z = -80 µm, dark contrasted grid structure of the test specimen

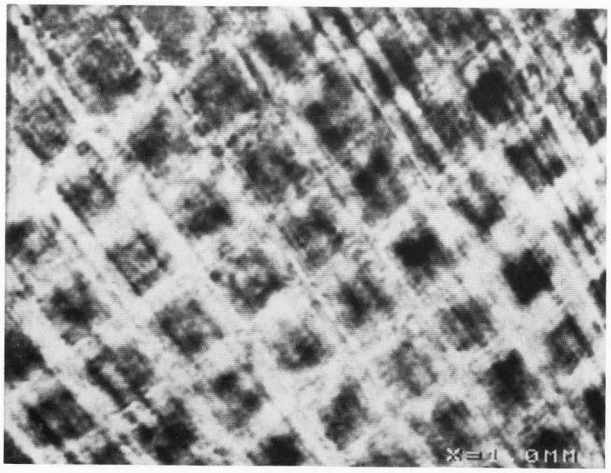

Fig. 4c z = -110 µm, bright contrasted grid structure of the test specimen

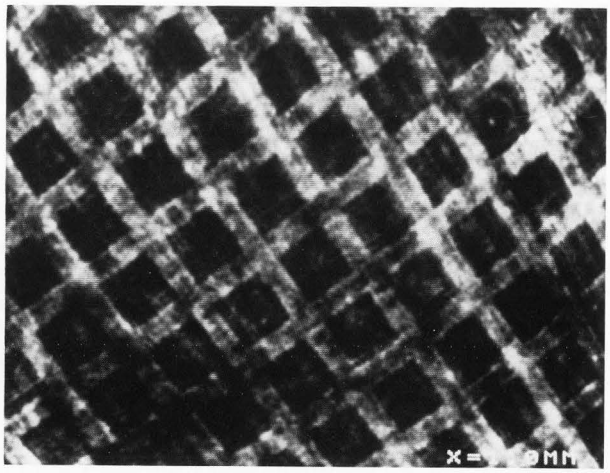

Fig. 4d z = -190 µm, bright contrasted and sharply contoured grid pattern

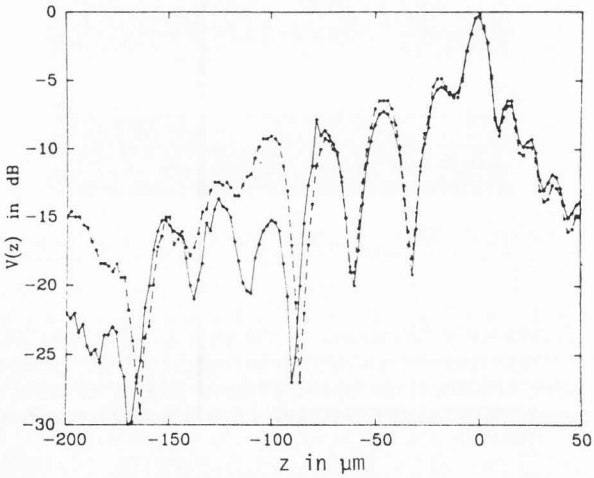

Fig. 5 Measured V(z)-characteristics:
$V_1(z)$ —— 30 µm aluminium over epoxy resin-composite
$V_2(z)$ --- 30 µm aluminium over 25 µm nickel mounted upon epoxy

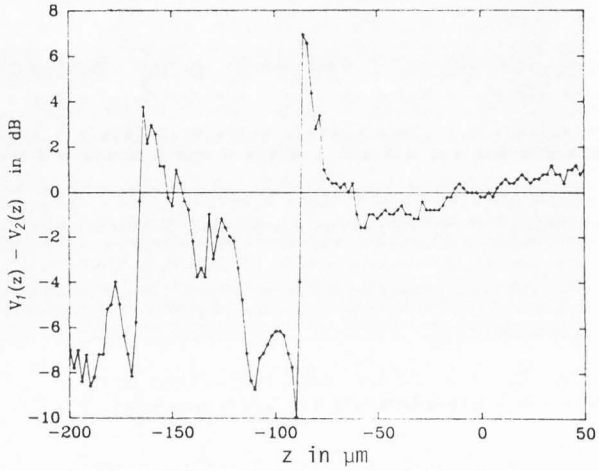

Fig. 6 Graph. $\Delta V(z) = V_1(z) - V_2(z)$

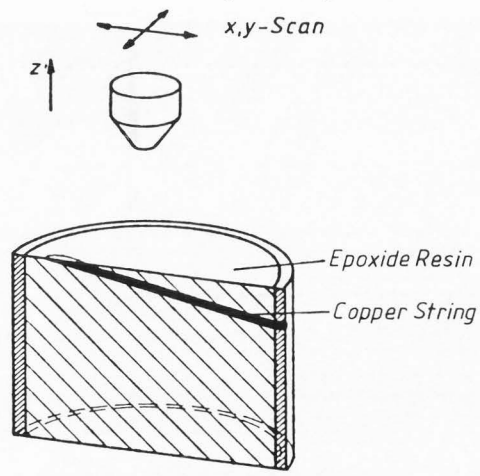

Fig. 7 Test specimen: embedded string

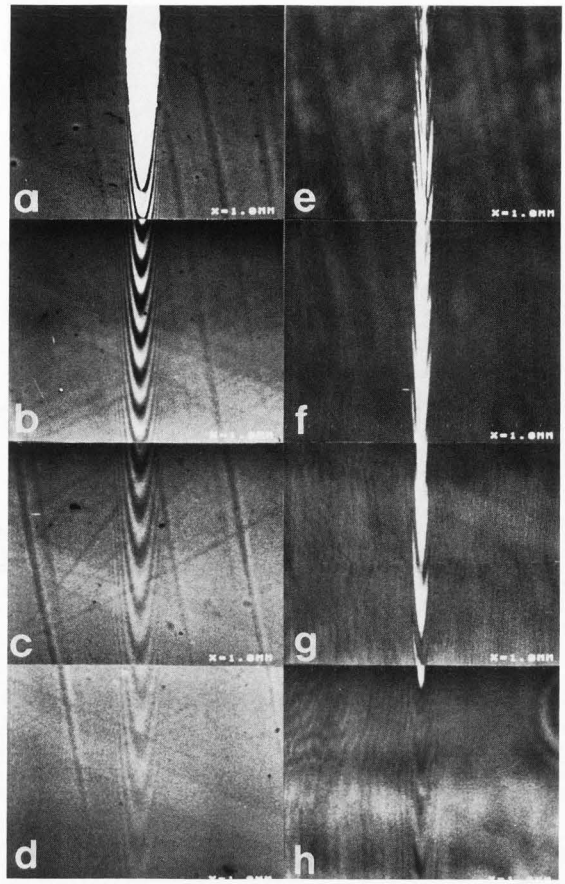

Fig. 8 Acoustic micrograph series of the recorded path of the copper string (Fig. 7).
Rod-diameter: 100 µm.
Series a-d: z = 0, e-h: z = -250 µm
(Area d and e are identical)
⊢⊣ = 100 µm

Focusing on the aluminium surface (**Fig. 4a**) enforces structural details of the surface like rippling and dot marks. A dark contrasted grid structure is visible after reduction of the gap between lens and surface to z = -80 µm (**Fig. 4b**). It should be noted that the contour of the grid is not sharply discernible. Inversion of the contrast is observed after lowering the distance to the surface to z = -110 µm (**Fig. 4c**). The best imaging conditions to observe structural details of the aluminium coated grid are found by a gap reduction to z = -190 µm (**Fig. 4d**). The grid lines are sharply contoured and the contrast conditions of the micrograph allow further detections of structural details by means of image analysis.

A first estimation of the contrast inversion gives the evaluation of the V(z) curves of these horizontal layered media: aluminium, nickel and epoxy resin. **Fig. 5** represents two characteristics both carried out by V(z)-profile of aluminium (30 µm) over epoxy resin. The broken plot (curve 2) figures the V(z)-intensities of the layered composite aluminium-nickel-epoxy resin.

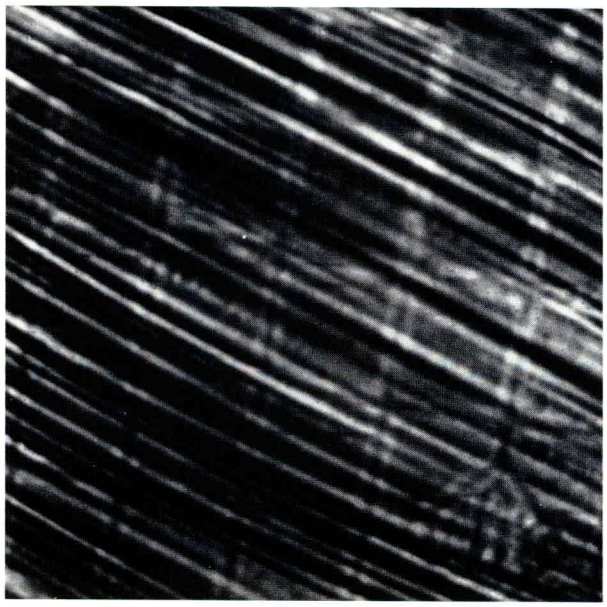

Fig. 9a SAM-micrograph of a mesh grid covered with a 60 µm-aluminium foil
⊢——⊣ = 100 µm

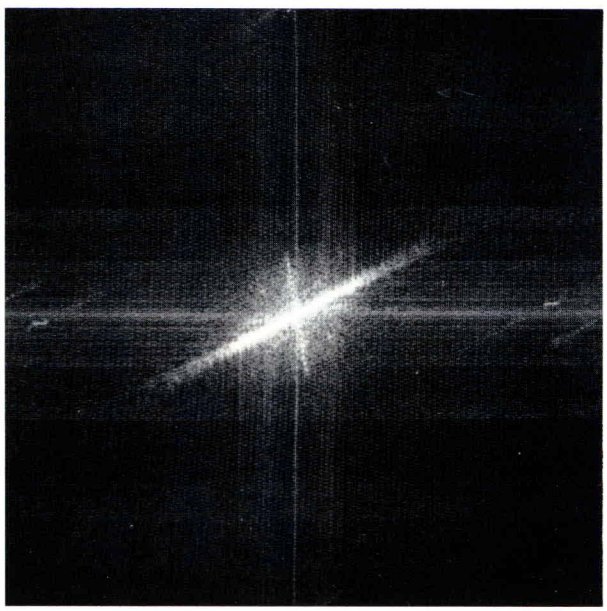

Fig. 9b Calculated mode of the Fourier-transformed spatial frequency distribution according to Fig. 9a

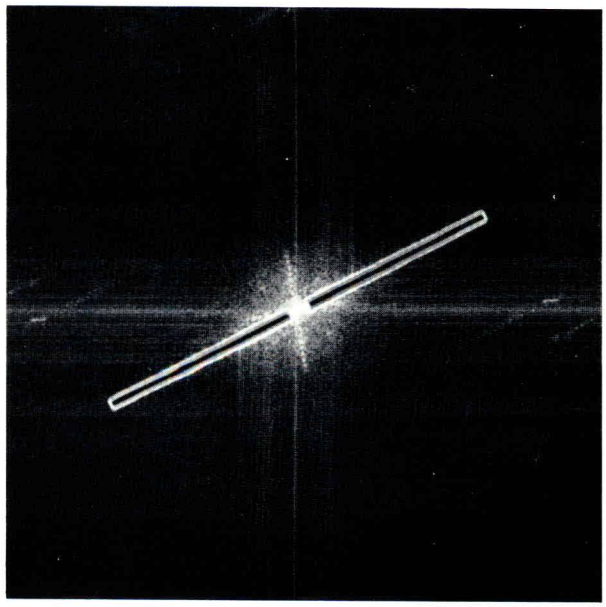

Fig. 9c Signal blanking in the frequency spectra of Fig. 9b

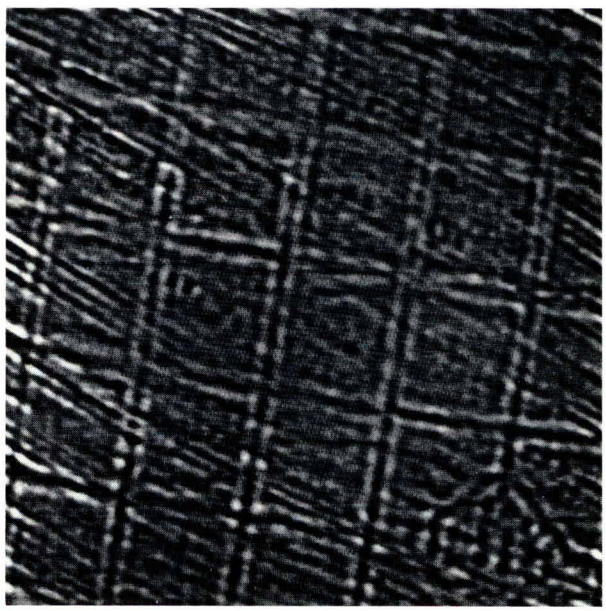

Fig. 9d Retransformed micrograph after frequency filtering
⊢——⊣ = 100 µm

The change in contrast below z = -75 µm is roughly observed by comparing both of these characteristics. A better discrimination was obtained by substracting the V(z)-values of curve 2 from those of curve 1 at corresponding depth values. The plotted difference profile Δ V(z) in **Fig. 6** indicates the observed contrast inversion at a depth of z = 88 µm. According to **Fig. 4b** the dark contrasted grid structure is due to positive signed ΔV(z)-values. The bright contoured grid pattern (**Figs. 4c, 4d**) corresponds with negative Δ V(z)-values.

Estimation of the Maximum Penetration Depth

Another point of interest is the determination of the maximum penetration depth of the reflected acoustic waves. The following experiment was useful to detect the penetration depth

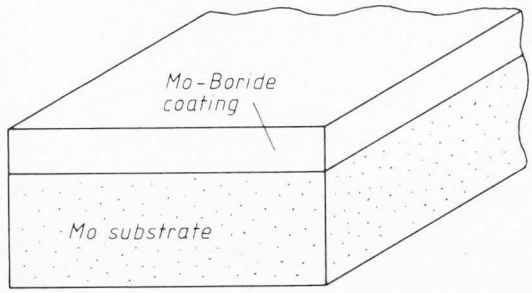

Fig. 10 Mo-boride coating on molybdenum

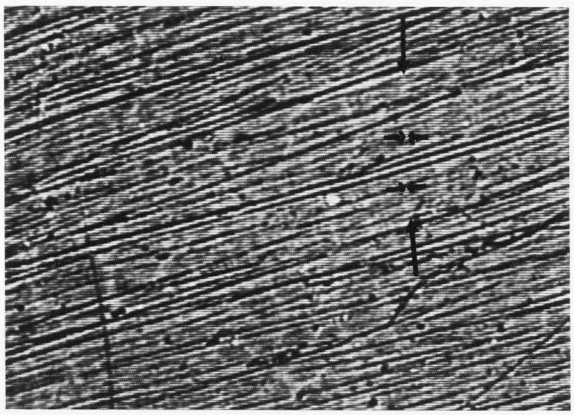

Fig. 11a SAM micrograph focused on the interface (crack marked with arrows)
⟷ = 100 µm

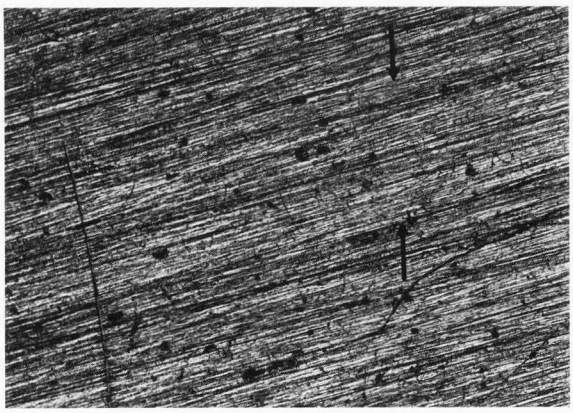

Fig. 11b Light optical micrograph of the corresponding surface area. Crack spacing (of Fig. 11a) marked with arrows
⟷ = 100 µm

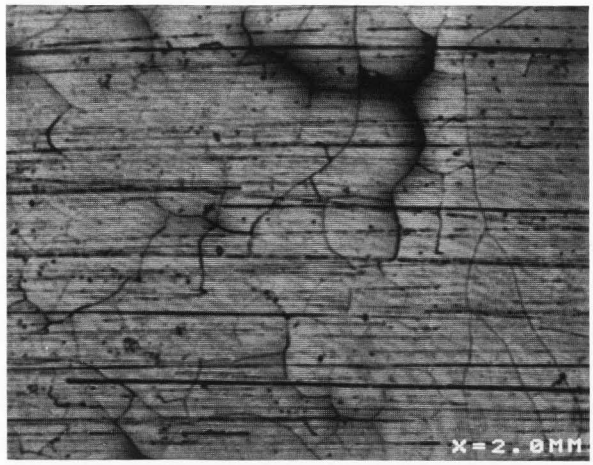

Fig. 12a Dark contrasted surface cracks on the coating, SAM micrograph (z=0)
⟷ = 100 µm

Fig. 12b Subsurface imaging at the same area (z=-20µm) shows additional bright contrasted crack-patterns
⟷ = 100 µm

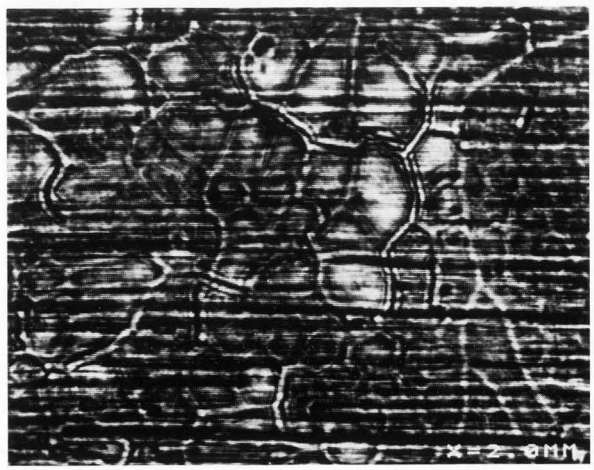

Fig. 12c SAM-micrograph corresponding to → Fig. 12a at z = -150 µm
⟷ = 100 µm

in epoxy resin. This was achieved by sequentially recording the substructural path of an inclined string embedded in epoxy resin (**Fig. 7**). The string was mounted on a cylindrical frame under an inclination angle $\alpha = 3°$. After embedding, the surface of the specimen was polished. The acoustical image of the rod is shown in the series (**Fig.8a-h**). Focusing on the surface ($z = 0$) shows the indepth path from the insertion down to a subsurface area (**Fig. 8a-d**). The reduction of the gap, surface-lens, to about 50 µm, i.e. $z = -250$ µm, results in the enhancement of the path (**Fig. 8e-h**). **Fig. 8d and 8e** represent the same area transmitted with different values of z($z = 0$, $z = -250$ µm). Sequentially monitoring leads to the detection limit (**Fig. 8h**), where the path disappears.

The total shift length (l) obtained during sequential mapping was used for the calculation of the penetration depth (d) with: $d = l.\tan\alpha$. For epoxy resin the estimated value was about 250 µm.

Image Analysis

The acoustomicrograph of the mapped transmitted and reflected acoustic signal contains all structural details detected during transition through the media. In many cases the determination of substructural details raises a lot of uncertainties. By use of image processing it is possible to suppress unsuitable structures superposed on the object of interest.

A method for erasing disturbing structures was achieved through the application of frequency filtering. **Fig. 9a** is the acoustomicrograph of a test specimen described above (**Fig. 3**). The object, a mesh grid (39.37 mesh per cm) was covered with a 60 µm cold rolled aluminium foil. This foil generates a superposed stripe-pattern due to the rippled surface.

Fig. 9b shows the spatial frequency pattern obtained by Fourier-transformation. The bright inclined diffraction-string, up from left to right, is due to the periodicity of the rippling marks (**Fig. 9a**). The spatial frequencies due to the shadowing stripes are blanked out as shown in **Fig. 9c**. The retransformed micrograph (**Fig. 9d**) shows the enhanced unshadowed grid structure.

Crack Detection in Surface Layers

A boride-layer on a molybdenum sheet (**Fig.10**) was examined by SAM. The 10 µm monophasic layer consists mainly of MoB_2. As predicted by various theories [3], cracking starts at the interface of the hard layer and the ductile substrate. By indepth focused acoustic wave monitoring a network of cracks is observed as a bright contrasted pattern (**Fig. 11a**). A comparison with light optical observations (**Fig. 11b**) proves that the cracks detected in **Fig. 11a** by means of SAM are below the surface.

Furthermore a specimen of the same type but loaded with surface cracks was tested by SAM (**Fig. 12a-c**).

The cracks detected by focal adjustment on the surface are dark contrasted (**Fig. 12a**). Subsurface imaging by indepth focused wave monitoring provides the detection of additional subsurface cracks (**Fig. 12b**). These crack patterns are bright contrasted and discernible from the surface cracks which remain dark contrasted at all imaging conditions. Much more reduction of the gap between lens and specimen leads to more information as shown in **Fig. 12c**. Some of the crack spacings are seamed with interference fringes due to diffractive properties [10]. These fringes are raised by interaction with surface waves. Therefore only surface cracks are decorated with fringes and can be distinguished from subsurface cracks. The bright areas centered in the cracking structure are probable due to separations of layer and substrate.

Conclusions

The detection of subsurface structures can be realized by means of SAM. The operating conditions, 200 MHz and distilled water as immersion medium, lead to a wide range of applications. Necessary information of the lateral resolution and the penetration depth are obtained by recording well known patterns with defined spacings. For calibrating the system, the implantation of test grids may be useful. As shown in the **Figs. 4-6**, the operating conditions for obtaining optimal contrasted mappings can be determined by plotting the V(z)-curves at different areas. These curves depend on the gap between lens and specimen in a significant manner and are very sensitive to elastic-material-parameters. The **Figs. 4 and 9** indicate that the subsurface-lateral-resolution seems to be less than 40 µm, which is the string-diameter of the test-grid-lines. These features may be a basic tool to determine quantitatively the structural details due to preselected analysis depths. To obtain information about the interface between coatings and base material when testing coated parts by means of SAM the evaluation of the contrast-conditions at various depths is necessary. This can be realized either by standard material calibrations or by computer aided calculations of the V(z)-characteristics, if the materials constants due to sound transmission are available.

Summary

Scanning acoustic microscopy (SAM) has been tested for the characterization of subsurface structures. The intention of the investigation was the non-destructive testing of thin surface coatings as used for metals protection. Therefore it was necessary to obtain two important informations which characterize the validity of the SAM-system at working conditions of 200 MHz and distilled water as immersion medium. These conditions are chosen because of simple experimental arrangements gaining sufficient resolving power.

To obtain the penetration depth of the ultrasound waves in metallic materials a specially developed specimen was tested. This horizontal layered composite consists of an aluminium coating and a nickel grid mounted below the aluminium-foil. The grid detection at various steps of in-depth analysis showed the depth-dependence of the

contrast conditions. The material-dependent contrast conditions are due to the spacing of lens and specimen as shown by a series of acoustomicrographs. A comparison with the corresponding V(z)-characteristics indicated the existence of contrast inversion due to the focusing depth. The maximum penetration depth of 250 µm was obtained by measuring the path length of an inclined string embedded in epoxy resin.

The erasing of unsuitable structures was realized by use of frequency filtering. As shown for example the hidden gridstructure shadowed by the surface pattern of a rippled aluminium coating was restored by means of this technique.

Surface examination of boride coated molybdenum by SAM demonstrated the detectability of subsurface cracks at the interface of layer and substrate. The contrast-inversion and the interference fringes on surface cracks allow the separation of subsurface cracks.

References

1. Atalar A.(1978). An angular spectrum approach to contrast in reflection acoustic microscopy. J. Appl. Phys. 49(10) 5130-5139

2. Bray RC, Quate CF, Calhoun J., Koch R.(1980). Film adhesion studies with the acoustic microscope. Thin Solid films 74 295-302

3. Ebert LJ, Krotine FT, Trojano AR(1967). Das Bruchverhalten einsatzgehaerteter Teile. Haerterei- Techn. Mitt. 22(2), 115-122

4. Jipson VB(1979). Acoustic microscopy of interior planes. Appl. Phys. Lett. 35(5) 385-387

5. Lemons RA, Quate CF(1979). Acoustic Microscopy, in: Phys. Acoust., Mason WP, Thurston RN (ed.), Academic Press NY 1979, 2-92

6. Matthaei E, Schulz A, Luebben Th, Boseck S, Vetters H, Mayr P(1984). Investigation of imaging with the scanning acoustic microscope. Sonderbaende der praktischen Metallographie 16, Dieser K, Kopp WU, Vetters H(ed.), Dr. Riederer Verlag, Stuttgart(1985), 43-51

7. Quate CF, Atalar A, Wickramasinghe HK(1979). Acoustic microscopy with mechanical scanning - a review. Proc. IEEE 67, 1092-1114

8. Somekh MG, Briggs, GAD, Ilett C(1984). The effect of elastic anisotropy on contrast in the scanning acoustic microscope. Phil. Mag. A 49(2), 179-204

9. Scanning Acoustic Microscope. (Report from Olympus Corporation of America, NY) (1982). Solid State Techn. October 1982, 119-120

10. Yamanaka K, Enomoto Y(1982). Observation of surface cracks with scanning acoustic microscope. J. Appl. Phy. 53(2), 846-850

Discussion with Reviewers

H. Hafsteinsson: How can you focus on the aluminium foil at the same time as you change the gap size?

Authors: In the experiment one obtains the maximum output signal when the focus of the acoustic beam lies approximately on the surface of the specimen. This position is defined by the value z=0. Atalar's theory shows that the geometrical paraxial focus does not correspond to that point of maximum signal detection (depending on the material of the specimen this difference can reach some microns at a working frequency of 200 MHz). While focusing into the object, i.e. changing the gap to negative z-values, the beam is disturbed by overlapped structures in a lower depth than the focusing "plane" of the reflected acoustic wave. Especially structures close to -or in- the surface raise superposed structures which suppress the signal of interest. The reason why surface structures then appear to be sharp is not totally understood yet. It might be the change in the gap size due to the roughness of the surface raising this effect. As you see in the V(z)-curves (**Fig. 5**), there is a high gradient at many values of z. That produces an additional contrast between the heights and depths due to the rippled surface (**Fig. 9a**).

H. Hafsteinsson: Why is the path enhanced at z = -250 microns when you measure the penetration depth?

Authors: The real distance between lens tip and focus in our system is about 300 µm (gap between lens tip and surface at z = 0). To prevent failures in analysis, a safety distance of 50 µm should be left. A longer distance would be better for subsurface imaging but the path through the coupling medium (water) and therefore the absorption conditions of ultrasound would cause problems in the case of surface focusing. The values of z and the detected penetration limit correspond only for epoxy resin and water. In other cases one would obtain different values of z and the penetration depth observed.

H. Hafsteinsson: According to **Fig. 6** shouldn't you get the best images at -90, -110, -160 and -180 microns?

Authors: Fig. 6 gives information about the expected contrast in the images. From this point of view the marked z- positions would give the best results. But the difference curve (**Fig.6**) gives no information about the sharpness of the test structure. The images in **Fig. 4** are pointed out from a focusing series (z=0 to z=-230 µm) in steps of 10 microns. By use of this series, **Fig. 4d** seems to be the best result concerning the contouring of the grid pattern.

G.A.D. Briggs: Please explain in detail the different theories of formation of contrast in the scanning acoustic microscope.

Authors: A theoretical discussion of the V(z)-curves was done by Atalar [1]. This theory explains that the output signal V(z) in the acoustic microscope depends on the geometrical and elastical (acoustical)parameters of the system (transducer, lens, immersion liquid, sample). Furthermore the formula described in this paper correlates the V(z)-output with the acoustic field of the transducer and the reflective function of the specimen by an integration over the transducer area. Reflective functions for different matter have been calculated by various authors (e.g. L.M. Breskovskikh, "Waves in layered

media" Academic Press (1980); T. Kundu, A.K. Mal, R.D. Weglein, J. Acoust. Soc. Am. 77 (2), 353-359). Based upon Atalar's formula we have developed a computer program for the calculation of the reflective function of a system of horizontal layered isotropic media. Corresponding to **Fig. 5**
(1) water-(30 µm)aluminium-epoxy resin
(2) water-(30 µm)aluminium-nickel.
The results obtained are plotted in the following V(z)-indepth characteristics (**Fig. 13**). The solid line (system 1) is in good correspondence with the measured curve in **Fig. 5** regarding the negative z-values. The different locations of the minima might result from deviations in the materials parameters (density, longitudinal and transversal sound velocity, attenuation of the wave modes in each component, thickness of the layer). The broken line (system 2) shows more differences to

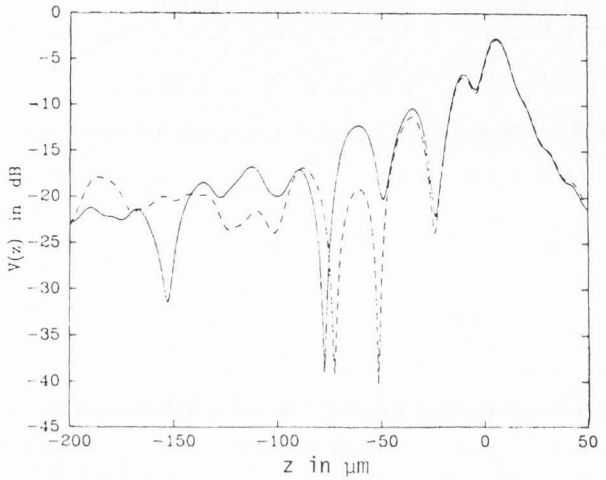

Fig. 13 **Calculated V(z)-curves: solid line: (30 µm-)aluminium-epoxy resin, broken line: (30 µm-)aluminium-nickel**

the measured characteristic (**Fig. 5**). Our opinion is, supported by our calculations that only the elastic parameters are involved in a good approximation while forming the V(z)-characteristics. The calculated plots are obtained by limiting the geometrical conditions. Therefore the theory implicates the horizontal infinite extension of the layered composites. By use of this model vertical boundaries are not taken in consideration.

Suggested Further Reading

Attal J (1980). Acoustic Microscopy: Imaging microelectronic circuits with liquid metals. In: Scanned Image Microscopy. Ash EA (Ed.), Academic Press 1980 97-118.

Hollis RL, Hammer R (1980). Defect detection for microelectronics by acoustic microscopy. In: Scanned Image Microscopy, Ash EA (Ed.) Academic Press 1980, 155-164.

Hoppe M, Atalar A, Patzelt WJ, Thaer A (1983). Leitz Akustomikroskop ELSAM. Anwendungen in der Materialuntersuchung-erste Ergebnisse. Leitz - Mitteilungen, Wissenschaft und Technik 8(5), 125-131.

Ilett C, Somekh MG, Briggs GAD (1984). Acoustic microscopy of elastic discontinuities. Proc. Royal Soc. A (London) 393, 171-183.

Kulakov MA, Mozorov AI (1983). Acoustic microscope visualization of the subsurface structure of objects. Sov. Techn. Phys. Lett (USA) 8(6),311-312.

Parmon W, Bertoni HL (1979). Ray interpretation of material signature in the acoustic microscope. Electron Lett. 15(21), 684-686.

Quate CF (1980-81). The acoustic microscope: a concept for microscopy using waves of sound. Nav. Res. Rev. (USA) 33(1), 24-32.

Weaver JMR, Briggs GAD, Somekh MG (1983). Acoustic microscopy of ultrasonic attenuation. J. de Phys., Coll. C9, Supp. 12(44), 371-376.

Weaver JMR, Ilett C, Somekh MG, Briggs GAD (1985). Acoustic microscopy of solid materials. Metallography 18(1), 3-34.

Weglein RD (1979). A model for predicting acoustic material signatures. Appl. Phys. Lett 34(3), 179-181.

Wickramasinghe HK (1984). Contrast and imaging performance in the scanning acoustic microscopy. J. Appl. Phys. 50(2), 664-672.

Yin QR, Ilett C, Briggs GAD (1982). Acoustic microscopy of ferroelectric ceramics. J. Mat. Science 17, 2449-2452.